^{93}Zr developments at the Heavy Ion Accelerator Facility at ANU

Stefan Pavetich[1,‡], Alexander Carey[1], L. Keith Fifield[1], Michaela B. Froehlich[1], Shlomi Halfon[2], Angelina Kinast[1,3], Martin Martschini[1,4], Dominic Nelson[1], Michael Paul[5], Asher Shor[2], Johannes H. Sterba[6], Moshe Tessler[5], Stephen G. Tims[1], Leonid Weissman[2], and Anton Wallner[1]

[1] Department of Nuclear Physics, Research School of Physics and Engineering, The Australian National University, 2601, Canberra, Australia

[2] Soreq Nuclear Research Center, Yavne, Israel 81800

[3] Fakultät für Physik, Technische Universität München, 85747 Garching, Germany

[4] University of Vienna, Faculty of Physics – Isotope Research and Nuclear Physics, VERA Laboratory, 1090 Vienna, Austria

[5] Racah Institute of Physics, Hebrew University, Jerusalem, Israel 91904

[6] Atominstitut, Technische Universität Wien, 1020 Vienna, Austria

[‡]Corresponding author: stefan.pavetich@anu.edu.au

Keywords: AMS; ^{93}Zr; neutron capture cross sections; isobar suppression

Abstract

The long-lived radionuclide ^{93}Zr $t_{1/2} = (1.61 \pm 0.05)$ Ma plays an important role in nuclear astrophysics and nuclear technology. In stellar environments, it is mainly produced by neutron capture on the stable nuclide ^{92}Zr. On Earth high amounts of radioactive ^{93}Zr are produced in nuclear power plants directly from ^{235}U fission, but also by neutron capture on ^{92}Zr, as Zr-alloys are commonly used as cladding for nuclear fuel rods.

Despite its importance, the neutron capture cross section of ^{92}Zr at thermal and stellar energies (keV) is not well known. Neutron irradiation of ^{92}Zr and subsequent determination of produced ^{93}Zr via AMS is a promising approach to resolve this issue. The main challenge in AMS measurements of ^{93}Zr is the interference from the stable isobar ^{93}Nb. The high particle energies available with the 14UD tandem accelerator at the Australian National University are ideal to tackle this challenge. Different sample materials, molecular ion species and sample holder materials were tested for their ^{93}Nb background. Commercial ZrO_2 powder irradiated with

thermal neutrons from the reactor at the Atominstitut in Vienna (ATI) was used as reference material for AMS measurements. In contrast to literature reports and γ-activity measurements of ^{95}Nb, which suggest that chemical Nb reduction works, elevated ^{93}Nb contents were measured in chemically pre-treated samples. The reasons are under investigation. At the ANU we developed AMS for ~210 MeV ^{93}Zr ions using an 8 anode ionisation chamber. We achieved background levels of ^{93}A/Zr~10^{-12} with acceptance of 2 to 8% of the ^{93}Zr ions at the high-energy side. This is more than an order of magnitude better than previously reported. The ^{93}Nb isobar was suppressed by a factor between 13,000 and 90,000 in the detector.

This performance allows measurements of the thermal and stellar neutron-capture cross section of ^{92}Zr for samples irradiated at the ATI and the Soreq Applied Research Accelerator Facility, respectively, using AMS.

1. Introduction

The 14UD (units doubled) pelletron accelerator at the Heavy Ion Accelerator Facility (HIAF) of the Australian National University (ANU) is one of the largest operational tandem accelerators. Terminal voltages of >14 MV are achieved regularly and allow AMS measurements of medium-mass isotopes at energies above 200 MeV. Measurements of ^{60}Fe/Fe and ^{53}Mn/^{55}Mn-ratios are undertaken routinely down to 10^{-17} [1] and 10^{-13} [2] levels, respectively.

The element Zirconium has 5 stable isotopes (^{90,91,92,94,96}Zr). The long-lived ^{93}Zr ($t_{1/2}$ = 1.61±0.05 Ma) [3] decays via β^- emission to the ground state (27±6)% and first excited state ((30.77±0.02) keV (73±6)%) of its stable isobar ^{93}Nb. The γ-transition from the first excited to the ground state is very weak with an intensity of only (4.3±0.4)×10^{-4}% [3]. This, together with the long half-life of ^{93}Zr, makes the determination of ^{93}Zr contents by decay counting extremely difficult. AMS represents an alternative method, provided background (i.e. the suppression of the interference from the stable isobar ^{93}Nb) can be controlled. The small relative difference in nuclear charge of $\Delta Z/Z = 1/40$ makes the separation of the isobar very challenging. Additional background may be introduced by the two stable neighboring isotopes ^{92}Zr and ^{94}Zr.

One interesting application of ^{93}Zr AMS is nuclear astrophysics. In stellar environments Zr-isotopes are predominantly produced by the slow neutron capture process (*s*-process) which takes place in the late phases of stellar burning [4-8]. Neutron capture cross sections are the key variables to model these astrophysical processes. They are of particular interest in the mass region between 90-100 amu as this is the matching point between two components of the

s-process, taking place in different stellar environments [4, 7, 9-11]. To date, all measurements of the cross section for $^{92}Zr(n,\gamma)^{93}Zr$ are based on the time-of-flight method [6, 12-16] and significant uncertainties remain. Using activation and subsequent AMS measurement of the reaction product provides an independent method with different systematic uncertainties [17-20]. In nuclear reactors, ^{93}Zr is a high-yield fission product and is also produced via neutron capture on ^{92}Zr present in the Zr-alloys used for cladding nuclear fuel rods. Spontaneous fission of naturally occurring Uranium and Thorium produces ^{93}Zr as well. Consequently, ^{93}Zr can be present in the environment and could be useful as a tracer in geological processes, tracing ocean currents, and for characterization of radioactive waste.

Previous work on AMS measurements of ^{93}Zr was predominantly undertaken at large tandem accelerators. The CIAE group at the 13 MV HI-13-AMS facility in Bejing achieved detection limits of $<10^{-10}$ for $^{93}Zr/Zr$ by extracting ZrO^- beams from ZrO_2 targets and using a multi-anode ionization chamber [21]. This limit was reached with ion energies of ~90 MeV. At the 14 MV MP Tandem at the Maier-Leibnitz-Laboratory at the Technical University Munich (TUM) two different isobar suppression methods have been tested: (i) a passive absorber and (ii) a gas filled magnet (GFM). Both methods were coupled with time-of-flight measurements [22] for $^{92,94}Zr$ isotopic identification, resulting in upper limits of $\sim10^{-9}$ for the $^{93}Zr/Zr$-ratio at ion energies between 150 and 200 MeV [22]. Recent work at TUM has further improved their sensitivity to $^{93}Zr/Zr$ $\sim5\times10^{-11}$ [23]. At the 11 MV FN Tandem accelerator of the Nuclear Science Laboratory in Notre Dame a GFM in combination with a parallel grid avalanche counter and a multi-anode-ionization chamber were used for ^{93}Zr measurements. Under optimal conditions this facility estimates a $^{93}Zr/Zr$ sensitivity limit of $\sim10^{-10}$ at ion energies of ~155 MeV [24-26]. In contrast to the 11-14 MeV facilities and based on test measurements performed with the stable isotopes ^{94}Mo (Z = 42), ^{93}Nb (Z = 41) and $^{92,94}Zr$ (Z = 40) with energies of 28 MeV, Martschini et al. [27] estimated a similar detection sensitivity of $\sim10^{-10}$ for $^{93}Zr/Zr$ at the much smaller 3-MV facility at VERA (Vienna Environmental Research Accelerator).

At the ANU, the main goal for the development of AMS of ^{93}Zr is to achieve the required sensitivity for applications in nuclear astrophysics, with particular emphasis on nucleosynthesis of the heavier elements in the *s*-process. The temperatures in massive stars in the *s*-process phase correspond to energies of 5-100 keV. Neutrons are produced and thermalized, hence their energies follow a Maxwell-Boltzmann distribution that represents the temperature of the respective star. Irradiation facilities like LiLiT (Liquid Lithium Target) at SARAF (Soreq Applied Research Accelerator Facility) [28-30] can provide a high neutron fluence of $\sim10^{10}$ n s^{-1} cm^{-2} in the energy range of interest for stellar nucleosynthesis studies (typically

30 keV). At these neutron fluences, and using the Maxwellian Averaged capture Cross Section (MACS) of (37.8±3.0) mb [6] for a 30 keV Maxwellian neutron spectrum one would reach a $^{93}Zr/^{92}Zr$ isotope ratio of ~10^{-11}, in a reasonable irradiation time of 100 h.

Hence, there is a need for AMS sensitivity to be further improved to make ^{93}Zr measurements of such materials possible.

2. Experimental method at the ANU

Various sample materials were investigated for ^{93}Nb background event rates and to test the chemical Nb reduction based on procedures described in [26, 31, 32]. An overview of the sample materials and the metallic binders employed is given in Table 1.

The isobaric separation capabilities of two different detector setups, a dedicated 8-anode ionization chamber (IC-8) [33], and the Enge gas filled magnet (GFM) [34, 35] in combination with a four-anode ionization chamber (IC-4) [36] were thoroughly assessed [37]. Samples irradiated with meV neutrons (reference samples), blanks and a sample irradiated with keV neutrons were investigated to determine performance parameters of the HIAF AMS setup for ^{93}Zr. The following performance parameters were determined in these tests: (i) the normalization factor (*Nf)*, being the ratio between the known nominal and the measured $^{93}Zr/^{92}Zr$-ratio, (ii) the $^{93}Zr/Zr$ background ratio (blank value or sensitivity) measured on samples containing no (or negligible amounts) of ^{93}Zr and (iii) the Nb suppression given by:

$$^{93}Nb_{sup} = \frac{^{93}Nb_{tot}}{^{93}Nb_{Zr-Roi}} * \frac{1}{Nf} \quad (1)$$

Here $^{93}Nb_{tot}$ and $^{93}Nb_{Zr\text{-}Roi}$ are the total number of Nb events registered in the ionization chamber and the number of Nb counts surviving all gates in the final ^{93}Zr region of interest (ROI), respectively, measured on a blank sample.

2.1 Sample materials

Commercial high purity ZrO_2, ZrF_4 and ZrH_2 powders with natural isotopic abundance purchased from Alfa Aesar (see Table 1) were used to investigate the Nb content for different ion beams. The same ZrO_2 powder (labeled α-blank) was later used for assessing ^{93}Zr-AMS performance at HIAF. In addition 47.9 mg of the same material (labeled ATI-Zr-nat-C) was used for irradiation with thermal neutrons at the TRIGA Mark II reactor of the Atominstitut in Vienna (ATI) [38] to produce a reference material with a sufficiently high $^{93}Zr/Zr$ isotope ratio.

The material was irradiated for 7 h at a position in the reactor which provides 99% thermal neutrons producing ^{93}Zr via the reaction ^{92}Zr(n,γ) and resulting in a ^{93}Zr/^{92}Zr-ratio of $(2.2\pm0.7)\times10^{-9}$ [39]. The neutron fluence was determined by gold monitor foils and also by the activity of the short lived ^{95,97}Zr isotopes, simultaneously produced by neutron capture on the stable ^{94,96}Zr. The large uncertainty is dominated by the large uncertainty of the thermal neutron capture cross section on ^{92}Zr of (0.26±0.08) b [40].

A sample containing 34 mg of highly enriched $^{92}ZrO_2$ (93.80% ^{92}Zr) mixed with 170 mg of high purity Al was irradiated with a Maxwell-Boltzmann neutron spectrum of kT ~30 keV produced by the ^{7}Li(p,n)^{7}Be reaction at the LiLiT beamline at SARAF (SIR1 sample see Table 1). This material was analyzed for the determination of the neutron capture cross section of ^{92}Zr at stellar energies. Assuming a neutron fluence of $\sim1.5\times10^{15}$ n cm^{-2} for the irradiation the expected ^{93}Zr/^{92}Zr-ratio is $(5.6\pm0.4)\times10^{-11}$.

Most of the samples were pressed directly into standard NEC (National Electrostatic Corporation) sample holders in pure form, as oxides, fluorides or hydrides. Some samples were also prepared by mixing with high purity Ag or Al powders (see Table 1, for the Nb-count rate tests). Typical ZrX_n masses were between 3 and 9 mg and mixing ratios were: ZrO_2:Ag~1:1.5, ZrO_2:Al~1:0.6, ZrF_4:Ag~1:2 and ZrH_2:Ag~1:1.5. The SIR1 material was provided as a mixture of ZrO_2:Al~1:5 and first AMS test samples were pressed into sample holders without further treatment.

Some ZrO_2 material (α-blank and ATI-Zr-nat-C) was chemically pretreated according to the procedure described in section 2.1.1. In addition we also investigated ZrO_2 samples provided by the AMS group of the University of Notre Dame which underwent chemical pretreatment as described in [26] at their laboratory.

Different sample holder materials (Al and Cu) were also tested for their contribution to the Nb content in the extracted ion beam.

2.1.1 Chemical sample preparation

Two different chemical procedures for Nb reduction were investigated. The main differences were the use of different resins and that one method did not require the use of HF during the elution process.

The first approach is based on [26, 31]. Briefly, the samples were dissolved in 1-2 drops of 48% HF and then taken up in HCl in order to obtain a 9M HCl-0.05M HF solution. Ion exchange

columns (KONTES® DISPOSAFLEX® column, ID = 8mm, column length = 200 mm) containing 6 g of BioRad AG® 1-X8 (100-200 mesh, Cl^- form) per sample were conditioned with 20 mL of 9M HCl-0.05M HF. The dissolved samples were loaded onto the columns. The resins were then rinsed with 15 mL of 9M HCl-0.05M HF to elute Zr; whilst Nb is retained on the column. The eluants were evaporated to near dryness and for one sample the column chromatographic step was repeated for further purification. Fluorides in all samples were subsequently expelled by fuming with 15% boric acid and the boron was then removed by methanol. The samples were then taken up in MilliQ water, precipitated as hydroxides using 28% NH_4OH and combusted at 1100 ºC overnight to convert the $Zr(OH)_4$ to ZrO_2.

The second approach assessed, follows that of [32], and reduces the usage of HF significantly. After the dissolution of ZrO_2, the samples were taken up in 10M HCl. This solution was loaded onto 2 mL Eichrom® columns, containing 0.5 g UTEVA® resin (100-150 μm) per sample, pre-conditioned with 15 mL 10M HCl. The resins were then rinsed with 20 mL 9M HCl and Zr eluted with 20 mL 4M HCl, whereas Nb is retained. The column chromatographic step was again repeated for one sample. The Zr was precipitated from the eluent as hydroxide using 28% NH_4OH and combusted at 1100 ºC.

To quantify the Nb reduction in the chemical procedures the radioactive isotopes ^{95}Zr ($t_{1/2}$=(64.032±0.006) d) [41], produced during the neutron irradiation of ZrO_2 at ATI, and its daughter ^{95}Nb ($t_{1/2}$=(34.991±0.006) d) [41] were used. To this end their activities were determined from the 724 keV, 757 keV (^{95}Zr) and 766 keV (^{95}Nb) γ-transitions [41], using a calibrated high-purity Ge-detector.

2.1.2 ^{93}Nb count rate measurements

Using an NEC MCSNICS ion source, ZrO^-, ZrF_5^-, ZrH^- and ZrH_3^- ions were extracted from ZrO_2, ZrF_4 and ZrH_2 powder, respectively. Initially the ^{93}Nb count rates from unprocessed oxides, fluorides and hydrides were studied using IC-8. The ^{93}Nb event rates in the detector, normalized to the $^{92}ZrX_n^-$ current on the low-energy side, were compared for the different sample materials. In these initial tests the 13+ charge state was selected, but in all later tests and sample measurements the 14+ charge state was used (see section 2.2).

2.2 ^{93}Zr AMS setup

The ^{93}Zr-^{93}Nb separation and detection capabilities were determined for two detection setups: (i) IC-8 and (ii) IC-4 attached to the Enge GFM. For these measurements a ZrO^- beam was

injected. Propane at a pressure of ~100 mbar was used for IC-8. For the second setup including the GFM, the magnet chamber was filled with 3.5 mbar of nitrogen and IC-4 was filled with ~83 mbar of propane. The first two anodes are split diagonally which allows position and angle determination of the particles [2].

The results for the performance parameters given here are based on measurements from four beamtimes. Previous work at the ANU performed by Wacker et al. for ^{99}Tc [33] with the dedicated IC-8 demonstrated a high suppression of the isobar ^{99}Ru. Hence, we employed the same ionization chamber for our Zr measurements. ZrO_2 samples were used for these experiments because sample preparation was easier, or not necessary at all.

With ZrO_2 as sample material, ZrO^- currents of 500 nA were readily available. In order to keep Nb count rates in the detector low enough for acceptable dead time levels, however, the ionizer and the Cesium oven had to be run at low power (typically 70-80 W) and temperature (typically 80 °C), respectively. A sputter voltage of 5 kV was used for all measurements. These conditions provided ZrO^- currents between 10 and 100 nA. The particles were pre-accelerated to 155 keV, and mass-selected with a 90° magnet for injection into the 14UD accelerator. The typical terminal voltage for mass 93 was 14.15 MV. A combination of gas and foil stripping was employed at the terminal (for details see [42]) and the 14+ charge state was selected, resulting in a total ion energy of ~210 MeV. The interaction with the gas stripper (~2×10^{-3} mbar) dissociates the injected molecules, whereas the foil stripper yields the necessary high charge states. Using the 14+ charge state provides an additional 14 MeV of particle energy for ^{93}Zr-^{93}Nb discrimination, compared to the 13+ charge state (196 MeV) used in the first background measurements.

The charge state yield for $^{92}Zr^{13+}$ based on [43] at 14.15 MeV terminal voltage is 11.2% but drops to 4.7% for the 14+ charge state. In contrast to the calculated value we measured transmissions of 2.5-4.5% for the 14+ charge state between the Faraday cup at the entrance of the accelerator and the Faraday cup directly in front of the detector. The particle transmission between the analyzing magnet and the Faraday cup in front of the detector is 100%. The most probable explanation for changes in the transmission is a different beam tuning through the accelerator for different beamtimes. A Wien filter was used to purify the beam from isotopic interference.

Initially a 0.7 µm thick Mylar window was used for IC-8 but this was replaced by a 5x5 mm^2 and 50 nm thick SiN entrance window (Silson Ltd, Southam, UK) for later measurements. The propane gas used in the first two beamtimes was replaced by isobutane in later beamtimes [44].

Signals from attenuated ^{92,94}Zr beams in the detector were used to estimate the position of the energy loss peaks for ^{93}Zr for each anode. An effective way to reduce interference from ^{93}Nb is to exploit the difference in ranges for ^{93}Zr (Z = 40) and ^{93}Nb (Z = 41) in the detector gas (see Figure 1). By adjusting the detector gas pressure only a small fraction of 0.15-1.5% of the ^{93}Nb was allowed to reach the last anode of the detector (see Figure 1). In contrast, for ^{92,94}Zr ions having the same magnetic rigidity as ^{93}Zr, 45-80% of the ^{92}Zr and 6-36% of ^{94}Zr reached the last anode. Interpolation between ^{92}Zr and ^{94}Zr suggests that between 26 and 63% of the ^{93}Zr ions reached the last anode. The large variation stems from different detector settings in the individual beamtimes. Within a single beamtime the relative change in the fraction of ions reaching the last anode was constant within a few percent. Only events producing signals at the last anode, ΔE_8, were considered for further data evaluation. Gates on individual and summed signals in different combinations were used to improve the identification of ^{93}Zr. The signal from a test pulser was used to match the gains of the 8 individual anode energy loss signals to derive the sum signals. A gate on the sum of the first 7 anodes or the sum of all 8 anodes was used to identify isotopic background caused by ^{92,94}Zr ions. The best separation of ^{93}Nb and ^{93}Zr was achieved using gates on individual energy loss signals along with a 2-dimensional gate in the spectrum $\sum_{i=1}^{5} \Delta E_i$ versus ΔE_7 (with the above mentioned ΔE_8 threshold).

Typically, the ^{92,94}Zr currents were measured for 10 s each, followed by counting at mass A=93 for 300-1000 s and another ^{92,94}Zr current measurement. A computer script controlled switching between the different isotopes by changing the values for the injection magnet, the terminal voltage and the electrical field of the Wien filter. Switching times from one isotope to the next were in the order of 10 s.

3. Results and Discussion

3.1 Sample material tests

The detector count rates for A = 93, measured for different materials (oxides, fluorides and hydrides), and normalized to the respective $^{92}ZrX_n^-$ currents were used as a relative measure for the ^{93}Nb content in the beam. The results of these measurements are shown in Table 2. For hydrides (e.g.: $^{92}ZrH^-$ and $^{92}ZrH_3^-$), currents measured at the low-energy side after the injection magnet were corrected for isobaric interference from other ZrH_n^--molecules. It is worth to note,

that the $^{93}Nb/^{92}ZrX_n^-$ ratio depends on the ^{93}Nb content in the different sample materials as well as on the chemical composition of the samples. Table 2 suggests that in ZrF_5^- the Nb content is reduced by more than an order of magnitude compared to hydrides or oxides [37]. However, the fact that our ^{92}Zr enriched sample was in oxide form and the excellent performance of ZrO_2 in the ion source, in terms of stability of the ion source output and durability of the samples, led to the decision to use oxides as AMS sample material for the remaining tests. In subsequent measurements the ion source output was adjusted to keep the maximum ^{93}Nb detector count rate below 10,000 events/s, which would result in detector dead times in the order of 30%. In fact, in more than 75% of the measurements the count rate was below 3,000 events/s and detector dead times were kept at less than 10%.

For chemically untreated samples of natural isotopic composition the typical $^{92}Zr^{14+}$ currents were between 3 and 50 nA and count rates in the detector were usually 50-300 s^{-1} nA^{-1} (normalized to $^{92}Zr^{14+}$), or ~25-150 s^{-1} nA^{-1}, if normalized to $^{92}ZrO^-$. The ^{92}Zr enriched sample showed a higher count rate of ~750 s^{-1} nA^{-1} (normalized to $^{92}Zr^{14+}$).

Surprisingly, all samples which were chemically treated to reduce the Nb content showed much higher ^{93}Nb count rates of 3,000-10,000 s^{-1} nA^{-1}. This is 1-2 orders of magnitude higher than for untreated oxide samples. In contrast, the ^{95}Zr and ^{95}Nb γ-activity of the neutron-irradiated material (ATI-Zr-nat-C) suggests a reduction of ^{95}Nb by a factor of >400. Furthermore, the samples provided by the Notre Dame AMS group, which were reported to be low in Nb, gave ^{93}Nb count rates of ~400 s^{-1} nA^{-1}. Lu et al. [25] present $^{93}Nb/^{90}Zr$-ratios of 6×10^{-5} for untreated samples and 2.4×10^{-7} to 6×10^{-8} for chemically processed samples. In the case of the latter samples this corresponds to count rates between 80 and 270 s^{-1} nA^{-1} (normalized to $^{92}Zr^{14+}$ currents). This is roughly in agreement with our measured count rates from these samples and in the same range as our untreated ZrO_2 material. Whereas the results of [25] imply that the chemical procedures reduce Nb down to trace levels, our γ-activity measurements further indicate that Nb reduction also works on the microscopic level (reduction of ^{95}Zr content in the sample from ~10^7 atoms to ~10^4 atoms). This suggests that Nb might be reintroduced in subsequent sample preparation steps, after extracting it from the sample matrix. Despite thorough cleaning procedures, a potential source of ^{93}Nb could be the ion source itself (e.g. Nb is used as mixing powder for Be measurements). A second ion source at HIAF, a single cathode SNICS, where no macroscopic amount of Nb-sample material has been introduced in the past, however, yielded similar Nb count rates for unprocessed ZrO_2 samples as the AMS MCSNICS version. Finally the standard ionizer was replaced with a high purity Ta ionizer (Ta sheet from Goodfellow, purity: 99.99%), but again no reduction in the Nb count rates could be achieved.

Mixing of ZrO_2 with Al or Ag, during target preparation, which always bears the risk of additional Nb contamination, was found unnecessary, as the ZrO^- current from pure oxides was sufficiently high and the ion source behavior was stable over time. Sample holders made of Al gave lower ^{93}Nb count rates than Cu sample holders.

3.2 Results for the ^{93}Zr AMS performance

The expected positions of the energy loss signals from ^{93}Zr ions and their FWHM (full width at half maxima) were calculated by interpolation from attenuated ^{92,94}Zr beams. This was compared to the position of the measured energy loss signals for ^{93}Nb ions. The difference in the ^{93}Zr and ^{93}Nb peak positions relative to the FWHM of the peaks was used as a measure for the isobar separation. Only three signals from IC-4 (ΔE_3, ΔE_4 and E_{Tot}) could be used, all giving a ^{93}Zr-^{93}Nb peak separation of ~0.4 FWHM. IC-8 allowed to utilize 7-8 individual signals with separations of up to ~1.6 FWHM (see Figure 2). This leads to a significantly higher ^{93}Zr-sensitivity in IC-8, although the Nb count rates in IC-4 are ~10 times lower, due to the Nb suppression by the GFM. The main reason for the lower energy resolution of IC-4 is the energy loss of ~60 MeV [45] for ions of initially ~200 MeV in the GFM. This energy is not available for ion identification in the detector. Energy loss straggling in the two foils and the N_2-gas in the GFM additionally broadens the energy loss signals. Furthermore, the large size of the ion beam after the GFM requires a large entrance window and a different detector geometry that impacts on the energy resolution of the IC. However, it is not excluded that a dedicated state-of-the-art multi-anode IC after the GFM with position and angle information [36] could reach a ^{93}Zr-^{93}Nb separation comparable to the one of IC-8.

A comparison of the calculated energy loss for Zr and Nb using SRIM [45] (see Figure 1) with the measured values for IC-8 (see Figure 2) demonstrates that the SRIM calculation can only serve as a first approximation. The measured values indicate that the intersection of the two energy loss curves is probably over the 5th anode, whereas SRIM predicts the intersection over the 6th anode (see Figure 1). The calculated range of the ions, however, matches experimental results quite well.

Examples of spectra obtained from the neutron irradiated ^{93}Zr reference material (ATI-Zr-nat-C) and a blank (non-irradiated, same material) are shown in Figure 3. While no difference between the ungated spectra of the blank and the reference material is apparent, the applied gates allow a clear distinction between the two samples with a factor of ~290 between the respective measured ratios. The normalization factor from this measurement is 38, resulting in

a corresponding normalized blank $^{93}Zr/^{92}Zr$-ratio of ~8×10^{-12}. Most of the background is attributed to ^{93}Nb, with smaller contributions from ^{92}Zr. Masses 92, 93 and 94 appear very well separated in the total energy spectrum (see Figure 4, sum over all energy loss signals), when accepting only ions that arrive on the last anode. The total energy loss spectra also allow the determination of ^{92}Zr rates in the detector. These were usually in the range of 0.01-0.2 s^{-1} nA^{-1}. This shows that - in absence of a time-of flight measurement - an ionization chamber with a high energy resolution is a necessity for the discrimination of ^{92}Zr. This is especially the case at HIAF, where isotopic purification is achieved only by means of a Wien filter (i.e. without low-energy and high-energy electrostatic analyzers). Figure 4 demonstrates that the resolution of the total energy signals was better than 0.5% and that the total energy loss peaks for masses 92, 93, 94 amu, injected at the same magnetic rigidity, are separated by 2-2.5 FWHMs [44].

The results for the average normalization factors, blank values and ^{93}Nb suppression factors for the four beamtimes, are given in Table 3. Normalization factors were calculated from the average over all measurements on the ATI-Zr-nat-C reference material in the respective beamtime. The uncertainty of the normalization factors suggests a reproducibility of between 5 and 8% for one measurement series. Blank values were calculated from the sum of all counts measured on a blank and normalization to the reference material. The values for the ^{93}Nb suppression were calculated according to equation (1) using the average normalization factors and the blank value of the respective beamtime. The averaged background $^{93}Zr/^{92}Zr$ ratios were $(1.9\pm0.6)\times10^{-11}$ and $(6\pm1)\times10^{-12}$ for "wide" and "narrow" regions of interest, respectively. This corresponds to $^{93}Zr/Zr$-ratios of $(3.2\pm1.0)\times10^{-12}$ and $(1.1\pm0.2)\times10^{-12}$, respectively. The given uncertainties are the standard deviation of the mean blank value. The small standard deviation of the three values from the "narrow" ROI evaluation indicates good reproducibility. The ~30% uncertainty of the nominal ratio of the reference material, is not included here.

A sample with a $^{93}Zr/^{92}Zr$ isotope ratio of 10^{-11} corresponds to a ^{93}Zr count rate of ~0.0045 s^{-1} nA^{-1} in the detector. At typical ^{93}Nb count rates (50-750 s^{-1} nA^{-1}) a ^{93}Nb suppression factor between 11,000 and 170,000 is required to get a 1:1 relation between counted ^{93}Zr and ^{93}Nb events in the final ROI.

Similarly, a ^{92}Zr suppression factor of between 2 and 40 is required to get a 1:1 relation between ^{92}Zr and ^{93}Zr events. Our typical suppression for ^{92}Zr was between 500 and 1500 (based on the measured separation in the total energy), suggesting low or negligible interference for samples with $^{93}Zr/^{92}Zr$ ~10^{-11} or higher.

The low background level suggests that samples with $^{93}Zr/Zr$-ratios > 5×10^{-11} such as the sample produced at SARAF (SIR1) are within the range for measurements at the ANU. A first

measurement of the SIR1 sample gives a preliminary $^{93}Zr/^{92}Zr$-ratio of ~5.5×10^{-11}, in very good agreement with the expected ratio.

4. Conclusion and outlook

AMS of ^{93}Zr is being successfully developed at ANU and ^{93}Zr applications have become feasible. When extracting ZrO^- beams from ZrO_2 samples, $^{93}Zr/Zr$-sensitivities in the order of 10^{-12} were achieved, with a ^{93}Zr detector acceptance (fraction of ^{93}Zr ions accepted with all gates, inverse normalization factor) between 1.7 and 8.2%, depending on the experimental setup. This value is 1-3 orders of magnitude better than previously reported sensitivities at other facilities. The high energies of ~210 MeV at HIAF and a dedicated multi-anode ionization chamber with an energy resolution of better than 0.5% were crucial for this achievement. The significantly lower ^{93}Nb content in the beam of ZrF_5^- ions suggests that an even lower background level could be obtained using ZrF_4 samples. Highly variable ion source output makes the usage of ZrF_4 as sample material challenging, especially with a slow-switching measurement procedure as described in subsection 2.2, where the stable ion beam currents are only measured in intervals of several minutes. However, this possibility will be investigated in the future.

With present sensitivity and detector acceptance at HIAF, the measurement of the astrophysically important neutron capture cross section on ^{92}Zr becomes feasible. Dedicated measurements of the SIR1 sample material, and identical, but not irradiated blank material are planned for the near future.

The lack of a well-known $^{93}Zr/^{92}Zr$ reference material is still an issue for any ^{93}Zr AMS application. One possibility for the production of such a reference material would be to take advantage of the well-known fission yields for mass 93. Alternatively the $^{96}Zr(p,\alpha)$ reaction yields ^{93}Y which decays to ^{93}Zr with a half-life of ~10 h [3].

A remaining open question is the elevated ^{93}Nb background for chemically pretreated samples. The γ-activity measurements and independent results from other facilities suggest that the chemical procedures work. If the Nb background is originating predominately from the ion source it should be at similar levels for all the samples. We will continue to investigate whether ^{93}Nb is introduced back into the sample matrix in later steps of the sample preparation.

Acknowledgments

This work was supported by the Australian Research Council DP140100136. We thank P. Collon and the Notre Dame AMS group for their blank material to assess the Nb background.

References:

[1] A. Wallner et al., Nature 532 (2016) 69.

[2] T. Fujioka, L.K. Fifield, J.O. Stone, P.M. Vasconcelos, S.G. Tims, J. Chappell, Nucl. Instr. Meth. B 268 (2010) 1209-1213

[3] C.M. Baglin, Nucl. Data Sheets 112 (2011) 1163-1389.

[4] M. Buss, R. Gallino, G.J. Wasserburg, Annu. Rev. Astron. Astrophys. 37 (1999). 239-309

[5] C. Traveglio, R. Gallino, E. Arnone, J. Cowan, F. Jordan, C. Sneden Astrophys. J. 601 (2004) 864

[6] G. Tagliente et al., Phys. Rev. C 81 (2010) 055801

[7] F. Käppeler, R. Gallino, S. Bisterzo, W. Aoki, Rev. Mod. Phys. 83 (2011) 157-193

[8] G. Magkotsios, F.X. Timmes, M. Wiescher., Astrophys. J. 741 (2011) 78

[9] C.M. Raiteri, R. Gallino, M. Busso, D. Neuberger, F. Käppeler, Astrophys. J. 419 (1993) 207

[10] R. Gallino, C. Arlandini, M. Busso, M. Lugaro, C. Travaglio, O. Straniero, A. Chieffi, M. Limongi, Astrophys. J. 497 (1998) 388

[11] M. Lugaro, F. Herwig, J.C. Lattanzio, R. Gallino, O. Straniero, Astrophys. J. 586 (2003) 1305

[12] R.L. Macklin, J.H. Gibbons, Phys. Rev. 159 (1967) 1007.

[13] J.W. Boldeman, A.R. de L. Musgrove, B.J. Allen, Nucl. Phys. A 31 (1976) 269.

[14] A. de L. Musgrove et al., Neutron Physics and Nuclear Data for Reactors and other Applied Purposes (OECD, Paris, 1978), 449

[15] K. Ohgama, M. Igashira, T. Ohsaki, J. Nucl. Sci. Techn.42 (2005) 333

[16] G. Tagliente et al., Proceedings "Nuclei in the Cosmos-IX", Geneva/ Switzerland (2006), Proceedings of Science, PoS (NIC-IX) 227

[17] I. Dillmann et al., Phys. Rev. C 79, (2009) 065805

[18] A. Wallner, T. Belgya, M. Bichler, K. Buczak, I. Dillmann, F. Käppeler, C. Lederer, A. Mengoni, F. Quinto, P. Steier, L. Szentmiklosi, Phys. Rev. Let. 112, (2014) 192501

[19] A. Wallner et al., Phys. Rev. C 93, (2016) 045803

[20] A. Wallner et al., Phys. Rev. C 96, (2017) 025808

[21] H. Shen, S. Jiang, M. He, K. Dong, Y. Ouyang, Z. Li, Y. Guan, X. Yin, B. Peng, D. Zhou, J. Yuan, S. Wua, Nucl. Instr. Meth. B 294 (2013) 136-142

[22] K. Hain, Accelerator Mass Spectrometry Relevant for Nuclear Waste Transmutation (Master Thesis), TU Munich, 2011.

[23] K. Hain, B. Deneva, T. Faestermann, L. Fimiani, J.M. Gomez-Guzmán, D. Koll, G. Korschinek, P. Ludwig, V. Sergeyeva, N. Thiollay, submitted to Nucl. Instr. Meth. B 423 (2018) 42-48

[24] W. Lu, P. Collon, Y. Kashiv, M. Bowers, D. Robertson, C. Schmitt et al., Nucl. Instr. Meth. B 294 (2013) 392-396

[25] W. Lu et al., Nucl. Instr. Meth. B 361 (2015) 491-495

[26] W. Lu, The Development of ^{93}Zr-^{93}Nb Isobar Separation Technique for Future ^{93}Zr AMS Measurement, (Ph.D. thesis), University of Notre Dame, 2015

[27] M. Martschini, J. Buchriegler, P. Collon, W. Kutschera, J. Lachner, W. Lu, A. Priller, P. Steier, R. Golser, Nucl. Instr. Meth. B 361 (2015) 201-206

[28] G. Feinberg, M. Friedman, A. Krása, A. Shor, Y. Eisen, D. Berkovits, D. Cohen, G. Giorginis, T. Hirsh, M. Paul, A.J.M. Plompen, E. Tsuk, Phys. Rev. C 85 (2012) 055810

[29] S. Halfon, G. Feinberg, M. Paul, A. Arenshtam, D. Berkovits, D. Kijel, A. Nagler, I. Eliyahu, I. Silverman, Rev. of Scientific Instruments 84 (2013) 123507

[30] M. Tessler et al., Physics Letters B 751 (2015) 418-422

[31] K.A. Kraus, G.E. Moore, J. Am. Chem. Soc. 73 (1951) 9-13

[32] Sz. Osváth, N. Vajda, Zs. Stefánka, É. Széles, Zs. Molnár, J. Radioanal. Nucl. Chem. 287 (2011) 459-463.

[33] L. Wacker, L.K. Fifield, S.G. Tims, Nucl. Instr. Meth. B 223-224 (2004) 185-189.

[34] M. Paul, B.G. Glagola, W. Henning, J.G. Keller, W. Kutschera, Z. Liu, K.E. Rehm, B. Schneck, R.H. Siemssen, Nucl. Instrum. Methods A 277 (1989) 418-430.

[35] L. Gladkis, Development of AMS Techniques for ^{53}Mn and ^{236}U, (PhD thesis), The Australian National University, (2006).

[36]. G.T. Leckenby, Remodelling a multi-anode ionization chamber detector for accelerator mass spectrometry of ^{53}Mn, (Honours Thesis) The Australian National University, (2017)

[37] A. Carey, Refining methods for ultra-sensitive detection of Zirtconium-93, (Honours Thesis) The Australian National University, (2015)

[38] https://ati.tuwien.ac.at/reactor/EN/

[39] D. Nelson, Creating a $^{93}Zr/^{92}Zr$ Standard for Accelerator Mass Spectrometry, (Honours Thesis) The Australian National University, (2015)

[40] B. Pritychenko, S.F. Mughabghab, Nucl. Data Sheets 113 (2012) 3120-3144., extended version: arXiv:1208.2879v3 [astro-ph.SR] 11 Sep 2013

[41] S.K. Basu, G. Mukherjee, A.A. Sonzogni, Nucl. Data Sheets 111 (2010) 2555-2737

[42] L.K. Fifield, S.G. Tims, T. Fujioka, W.T. Hoo, S.E. Everett Nucl. Instr. Meth. B 268 (2010) 858-862.

[43] R.O. Sayer, Revue de Physique Appliquee 12 (1977) 1543-1546

[44]. M. Martschini, L.K. Fifield, M.B. Froehlich, G. Leckenby, S. Pavetich, S.G. Tims, B. Tranter, A. Wallner., Nucl. Instr. Meth. these proceedings

[45] available at: <www.srim.org>.

Table captions

Table 1: Overview of the materials studied in this work. The first four entries are materials used for the determination of the ^{93}Nb content in ^{93}Zr beams. The three later entries, all ZrO_2, are materials which were used for developing ^{93}Zr-AMS and evaluating our performance.

Table 2: Comparison of the $^{93}Nb^{13+}$ count rates normalized to $^{92}ZrX_n^-$ currents measured at the low-energy side of the 14UD accelerator.

Table 3: Normalization factors, blank values (sensitivity limits) and ^{93}Nb suppression factors for the individual beamtimes applying “wide” and “narrow” settings for the regions of interest.

Table 1

Sample name	Sample material (Supplier and purity)	Comment
ZrO_2	ZrO_2 Alfa Aesar, natural isotopic composition	used in pure form and as a mix with Ag (Alfa-Aesar 99.999% purity) and Al (Alfa-Aesar 99.97% purity)
ZrF_4	ZrF_4 Alfa Aesar, natural isotopic composition	used in pure form and as a mix with Ag (Alfa-Aesar 99.999% purity)
ZrH_2	ZrH_2 Alfa Aesar, natural isotopic composition	used in pure form and as a mix with Ag (Alfa-Aesar 99.999% purity)
Notre Dame ZrO_2	-	ZrO_2 blank material chemically processed at and provided by University of Notre Dame
α-blank ZrO_2	ZrO_2 Alfa Aesar, natural isotopic composition	Natural isotopic composition, used in pure form
ATI-nat-C	ZrO_2 Alfa Aesar, natural isotopic composition	α-blank irradiated with thermal neutrons at ATI, used in pure form
SIR1	ZrO_2 Isoflex (USA) enriched in ^{92}Zr (93.80%)	irradiated with keV neutrons at SARAF, mixed in a mass ratio of 1:5 with Al

Table 2

Selected molecule ZrX_n^-	$^{93}Nb^{13+}$ count rate $[s^{-1}]$	$^{92}ZrX_n^-$ current [nA]	$^{93}Nb^{13+}$ count rate normalized to current $[s^{-1}\ nA^{-1}]$
ZrO^-	10^{5} *	365	270
ZrF_5^-	300	64	5
ZrH^-	1300	27.7	47
ZrH_3^-	400	3.32	120

* Scaled from chopped beam.

Table 3

	Beamtime	Normalization factor	^{93}Zr/Zr blank value [10^{-12}]	^{93}Nb suppression factor [10^{4}]	Number of counts in ^{93}Zr ROI from blanks
Wide regions of interest	07/2016	15±1	2.1	1.3	37
	10/2016	12±1	5.5	1.2	167
	06/2017	25±2	4.1	2.8	23
	07/2017	32±2	1.1	2.7	23
Narrow regions of interest	07/2016	-	-	-	-
	10/2016	19±1	1.2	5.8	23
	06/2017	45±3	1.3	9	4
	07/2017	59±5	0.7	4.2	8

Figure captions

Figure 1: Energy loss curves for 210 MeV Zr and Nb ions in 98 mbar of propane according to SRIM. Interestingly, SRIM predicts a surprising double crossing in the energy loss of Zr and Nb, which suggests that these data are only indicative. The length of the individual anodes is indicated by lines. The average range of Zr ions is ~4 mm longer than for Nb ions.

Figure 2: Separation of the energy loss signals for ^{93}Zr and ^{93}Nb for three different detector settings of IC-8. The distance from the horizontal line at y = 0 gives the separation of the two peaks in units of FWHM. Negative values indicate that ^{93}Nb loses more energy at the respective anode and positive values mean ^{93}Zr is losing more energy.

Figure 3: Two dimensional energy loss spectra for measurements of α-blank and a reference sample (ATI-Zr-nat-C with ^{93}Zr/^{92}Zr~2.2×10^{-9}). The upper graphs show the ungated spectra, the lower graphs the same data gated on ΔE_8, ΔE_6 and E_{ALL} (sum ΔE_1-ΔE_8).

Figure 4: Total energy (sum over energy loss signals from all anodes) spectrum for IC-8. The spectrum is a superposition of three individual measurements, with settings for attenuated beams of ^{92,94}Zr and the setting for mass 93. Note the excellent energy resolution of better than 0.5%, which corresponds to a separation between neighboring masses of ~2 2.5 FWHM.

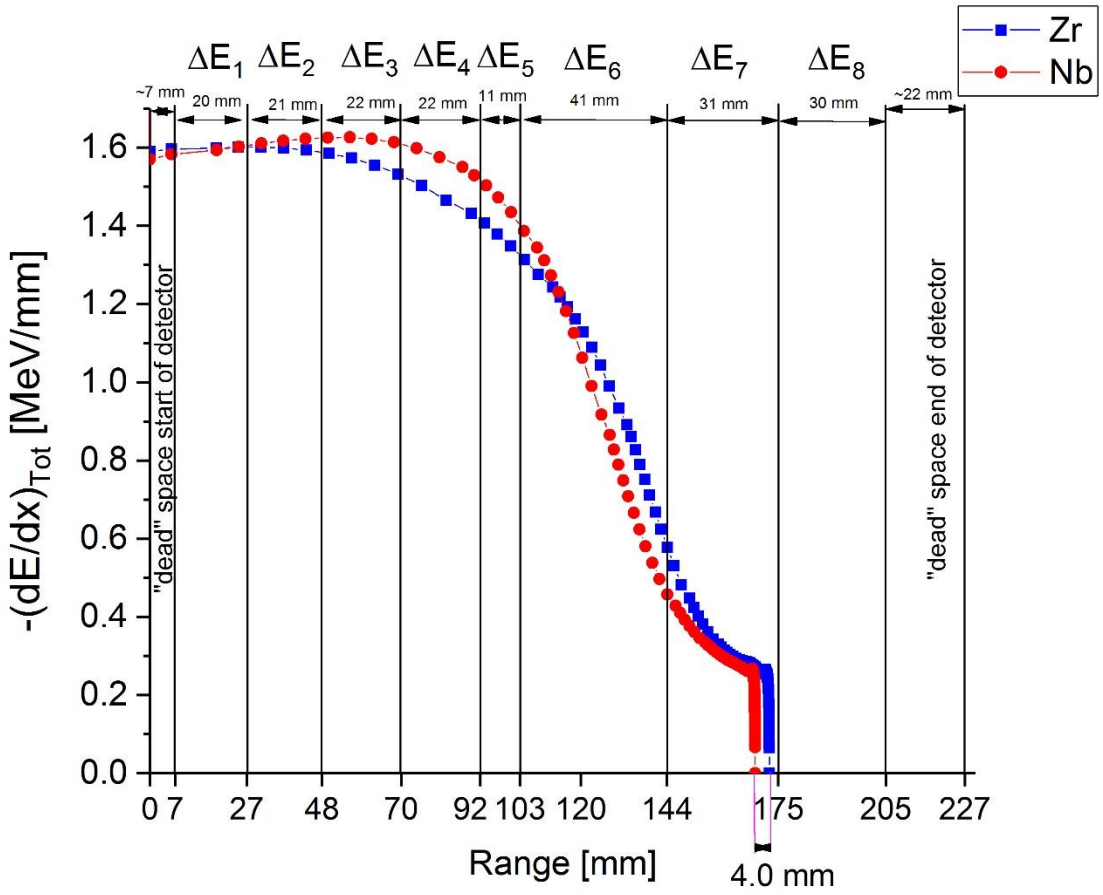
ΔE1 ΔE2 ΔE3 ΔE4 ΔE5 ΔE6 ΔE7 ΔE8
~7 mm
20 mm
21 mm
22 mm
22 mm
11 mm
41 mm
31 mm
30 mm
~22 mm
Zr
Nb
"dead" space start of detector
"dead" space end of detector
-(dE/dx)Tot [MeV/mm]
0.0
0.2
0.4
0.6
0.8
1.0
1.2
1.4
1.6
0 7 27 48 70 92 103 120 144 175 205 227
Range [mm]
4.0 mm

Figure 1

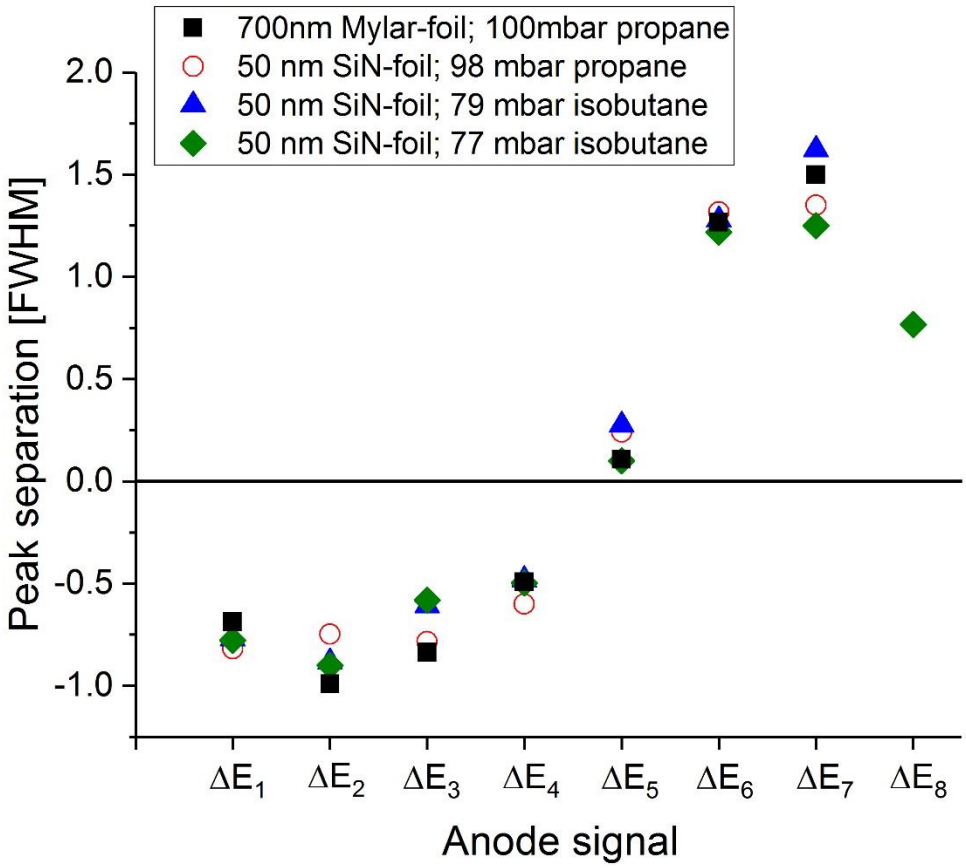
700nm Mylar-foil; 100mbar propane
50 nm SiN-foil; 98 mbar propane
50 nm SiN-foil; 79 mbar isobutane
50 nm SiN-foil; 77 mbar isobutane
Peak separation [FWHM]
2.0
1.5
1.0
0.5
0.0
-0.5
-1.0
ΔE1
ΔE2
ΔE3
ΔE4
ΔE5
ΔE6
ΔE7
ΔE8
Anode signal

Figure 2

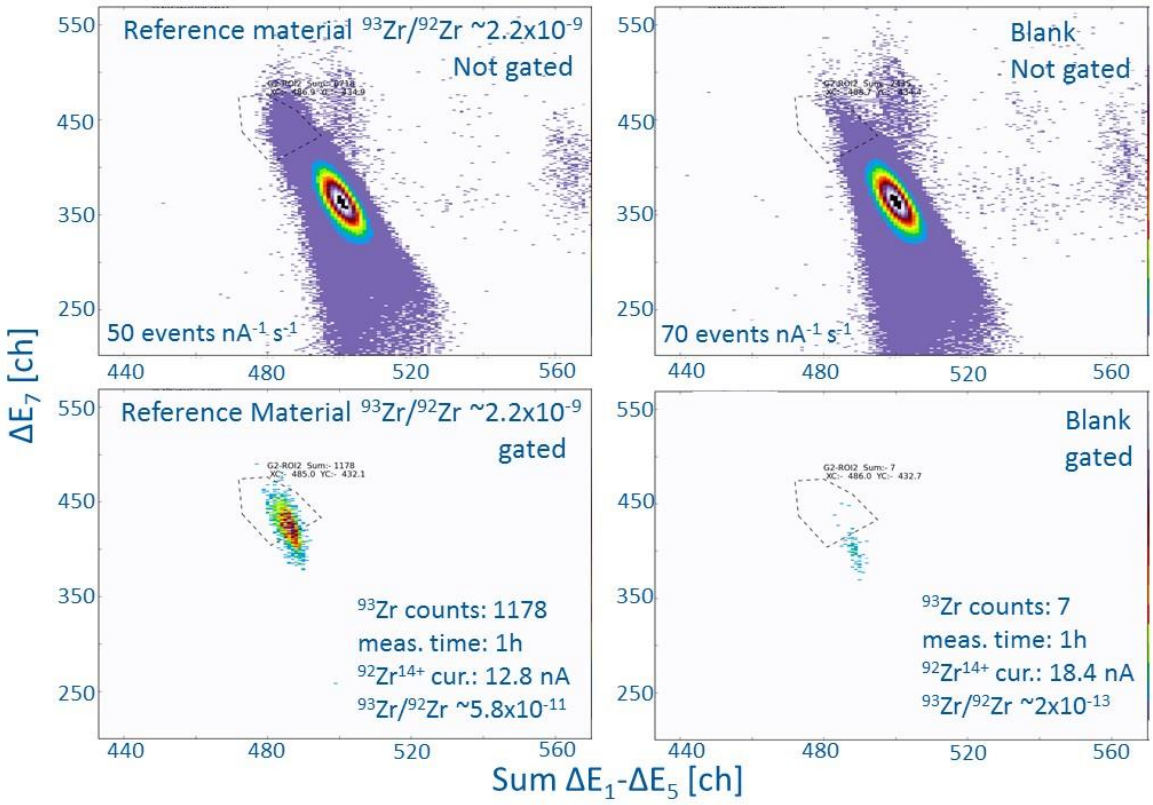
Reference material $^{93}Zr/^{92}Zr$ ~2.2x10^{-9}
Not gated
50 events nA^{-1} s^{-1}
Blank
Not gated
70 events nA^{-1} s^{-1}
Reference Material $^{93}Zr/^{92}Zr$ ~2.2x10^{-9}
gated
^{93}Zr counts: 1178
meas. time: 1h
$^{92}Zr^{14+}$ cur.: 12.8 nA
$^{93}Zr/^{92}Zr$ ~5.8x10^{-11}
Blank
gated
^{93}Zr counts: 7
meas. time: 1h
$^{92}Zr^{14+}$ cur.: 18.4 nA
$^{93}Zr/^{92}Zr$ ~2x10^{-13}
ΔE_7 [ch]
Sum ΔE_1-ΔE_5 [ch]
550
450
350
250
440
480
520
560

Figure 3

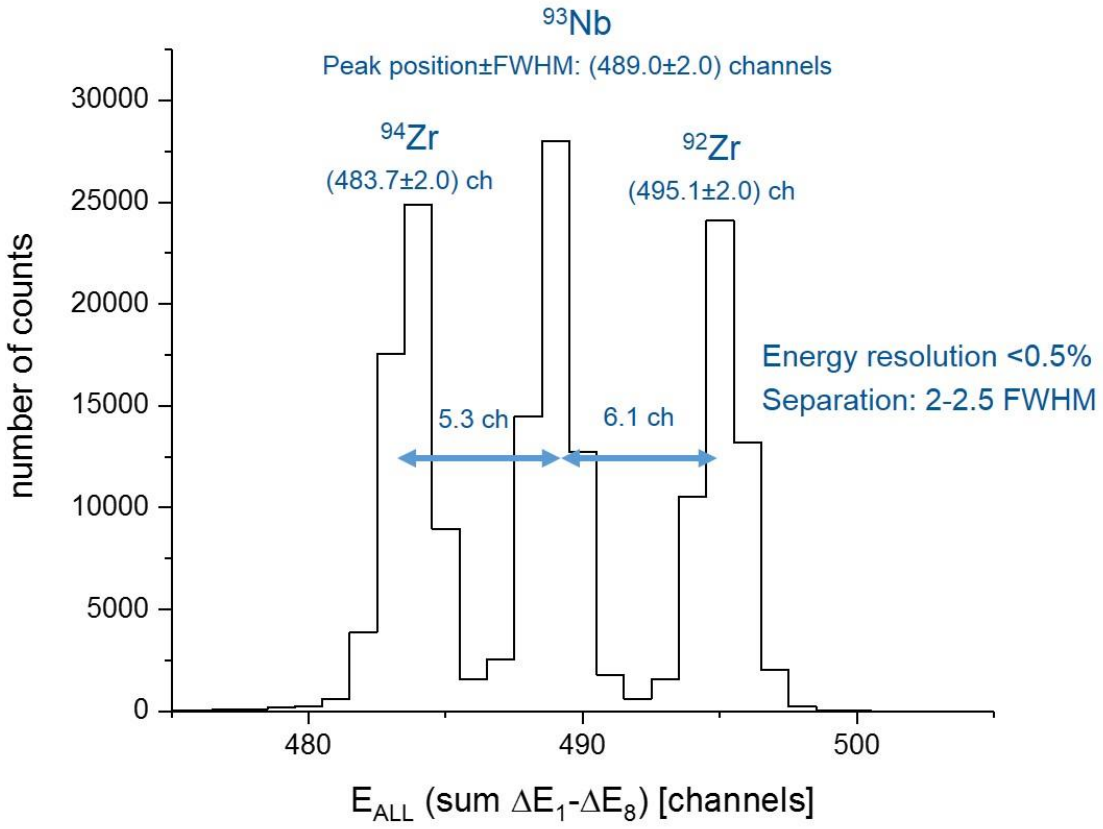
93Nb
Peak position±FWHM: (489.0±2.0) channels
94Zr
(483.7±2.0) ch
92Zr
(495.1±2.0) ch
Energy resolution <0.5%
Separation: 2-2.5 FWHM
5.3 ch
6.1 ch
number of counts
30000
25000
20000
15000
10000
5000
0
480
490
500
E_ALL (sum ΔE1-ΔE8) [channels]

Figure 4